A&A 616, L2 (2018)
https://doi.org/10.1051/0004-6361/201833647

Astronomy & Astrophysics

LETTER TO THE EDITOR

Planetary nebula distances in *Gaia* DR2⋆

S. Kimeswenger[1,2] and D. Barría[1]

[1] Instituto de Astronomía, Universidad Católica del Norte, Av. Angamos 0610, Antofagasta, Chile
e-mail: stefan.kimeswenger@gmail.com
[2] Institut für Astro- und Teilchenphysik, Leopold–Franzens Universität Innsbruck, Technikerstr. 25, 6020 Innsbruck, Austria

Received 14 June 2018 / Accepted 17 July 2018

ABSTRACT

Context. Planetary nebula distance scales often suffer from model-dependent solutions. Model-independent trigonometric parallaxes have been rare. Space-based trigonometric parallaxes are now available for a larger sample using the second Data Release of *Gaia*.
Aims. We aim to derive a high-quality approach for selection criteria of trigonometric parallaxes for planetary nebulae and discuss possible caveats and restrictions in the use of this Data Release.
Methods. A few hundred sources from previous distance scale surveys were manually cross-identified with data from the second *Gaia* Data Release (DR2) because coordinate-based matching does not work reliably. The data were compared with the results of previous distance scales and to the results of a recent similar study that used the first Data Release *Gaia* DR1.
Results. While the few available previous ground-based trigonometric parallaxes as well as those obtained with the *Hubble* Space Telescope perfectly match the new data sets, older statistical distance scales, reaching larger distances, do show small systematic differences. When we restrict the comparison to the central stars for which the photometric colors of *Gaia* show a negligible contamination by the surrounding nebula, the difference is negligible for statistical distances based on radio flux, while those derived from Hα surface brightness still show minor differences. The DR2 study significantly improves the previous recalibration of the statistical distance scales using DR1/TGAS.

Key words. astrometry – parallaxes – planetary nebulae: general

1. Introduction

The distances to planetary nebulae (PNe) have always faced the difficulty that nearby targets were lacking that could be reached well by direct methods. Trigonometric parallaxes have been obtained in a homogeneous long time-line campaign by the US Naval Observatory (USNO; Harris et al. 2007) and from the *Hubble* Space Telescope (HST; Benedict et al. 2009). Other studies (Acker et al. 1998; Smith 2015) showed that HIPPARCOS spacecraft parallaxes do not seem to be reliable. It was assumed that contamination by the emission of the surrounding nebulae caused these problems. Another model-independent method for distances to PNe are a cluster membership, as studied extensively by Majaess et al. (2007, 2014), and as discussed in Frew et al. (2016). In addition to these model-independent methods, a wide variety of statistical, model-dependent individual distance scales have been derived. The most frequently used of these are certainly those that are based on surface brightness versus angular sizes. They sometimes include optical depth corrections. All these methods have to be calibrated against a data set of nebulae with known distances. The older, widely used method is based on the 6 cm radio continuum flux, either using the ionized mass concept of Daub (1982) in the calibrations of Cahn et al. (1992) and Stanghellini et al. (2008), or by means of the radio continuum brightness temperature as used by van de Steene & Zijlstra (1994) and calibrated with a Galactic bulge sample. The newest model developed by Frew et al. (2016) is based on similar ideas, but makes use of the optical Hα surface brightness and a wide set of various calibrators. Moreover, they use a completely homogeneous data set for the brightness data derived earlier by themselves (Frew et al. 2013). Smith (2015) and Frew et al. (2016) described the underlying physics and assumptions for all these methods in detail. With the upcoming *Gaia* project (Gaia Collaboration 2016), a new era was expected to start for many classes of objects. The first step into this was described by Stanghellini et al. (2017) based on the combined *Tycho* + *Gaia* DR1 solution called TGAS (Michalik et al. 2015). With the second Data Release of *Gaia* (hereafter GDR2; Gaia Collaboration 2018), a complete homogeneous data set based only on *Gaia* measurements is available now for the first time. We present here the comparison of this new data set with common previous calibrations of PNe distances. Moreover, we compare it to the preliminary TGAS results in Stanghellini et al. (2017). Finally, we discuss possible caveats using the current GDR2.

2. Sample selection

The trigonometric parallaxes of the USNO data set (Harris et al. 2007) including 15 targets together with the HST parallaxes for 4 objects (Benedict et al. 2009) were selected. Based on the calibration of Stanghellini et al. (2008), the catalog of distances based on radio flux compiled by Stanghellini & Haywood (2010, Table 1; hereafter SH10) was used as input catalog and was combined with the distances based on optical Hα brightness

⋆ Table A.1 is only available at the CDS via anonymous ftp to cdsarc.u-strasbg.fr (130.79.128.5) or via http://cdsarc.u-strasbg.fr/viz-bin/qcat?J/A+A/616/L2

of Frew et al. (2016; hereafter FPB16). For the latter we employed the distances form their Table 12 using the general "complete sample" calibration. The *Gaia* data were taken interactively from the online data base using various search radii of up to 15″. This was necessary because the coordinates in the catalogs for older extended PNe are often not centered on the central star. We performed this for the 15 trigonometric parallaxes and for all 728 targets in SH10. We then compared the targets interactively in the Aladin Desktop Applet (Bonnarel et al. 2000). We used various sky survey plate scans from SuperCOSMOS (Hambly et al. 2001) and 2MASS (Skrutskie et al. 2006) and the help of finding charts like those in the ESO Strasbourg Catalogue of Galactic PNe (Acker et al. 1992) and in the HASH data base (Bojičić et al. 2017) for identification. However, in some cases of faint central stars, we also used the original literature, like Weinberger (1977) and Kwitter et al. (1988). Only targets with a secure identification match in order of magnitude and clear identification on finding charts as well were used as positive matches. In total, 382 out of the 728 sources from SH10 were matched. We found the blue central source for two targets for the first time. The complete data set with the cross identifications is given as electronic supplementary material. In the sample of 382 targets, many sources do have large formal (statistical) errors or even negative parallax values in the *Gaia* data base. Only 199 sources do have a formal error of $\sigma_\pi/\pi < 0.50$ (out of which 170 are listed also in FPB16). As expected from the typical error for an isolated star of 0.03–0.04 mas in the current Data Release (Luri et al. 2018), all sources beyond 4 kpc have errors larger than 0.25. Thus, we restricted our analysis to a sample below 4 kpc that was split into two subsamples for $\sigma_\pi/\pi < 0.15$ (81 sources from SH10, 75 of which are also listed in FPB16) and for $\sigma_\pi/\pi < 0.25$ (32 sources from SH10, 26 of which are also listed in FPB16). The analysis in the remaining paper focuses on these two subsamples, although we kept all sources in the online supplementary material to allow fast cross-identification with future releases (Table A.1).

3. Discussion

3.1. Trigonometric parallaxes

The trigonometric parallaxes, obtained with nearly 20 yr of ground-based observations at USNO (Harris et al. 2007), are currently the largest homogeneous reliable sample of that type (see Smith 2015; Frew et al. 2016). Four targets from this list have also been observed for slightly longer than three years with the HST (Benedict et al. 2009). All targets from the USNO list except for PHL 932, which was identified to be a compact H II region instead of a PN (Frew et al. 2010), were used here and are identified in GDR2. The parallaxes range from 1.3 to 8.0 mas (≈0.1–0.8 kpc) and have an average formal error of 3.2% in GDR2, which reaches 9% for one source. The USNO data set reports a mean error of 20% and a maximum error of 39%, while the four additional sources observed with the HST have a mean error of 10% and a maximum error of 17%. Figure 1 shows the USNO and HST trigonometric distances versus the GDR2 distances. Using only the USNO data, an almost 1:1 match is found, while the HST data tend to provide a slightly longer distance scale for distances exceeding 0.4 kpc. Although a scaling factor of 1.17 (median) between the USNO and HST parallaxes was found, Smith (2015) argued that the distance scales do not differ within the statistical errors because of the high scatter when comparing these two sets to each other. However, the higher accuracy of the *Gaia* data now shows that the HST data systematically deviate from the 1:1 relation.

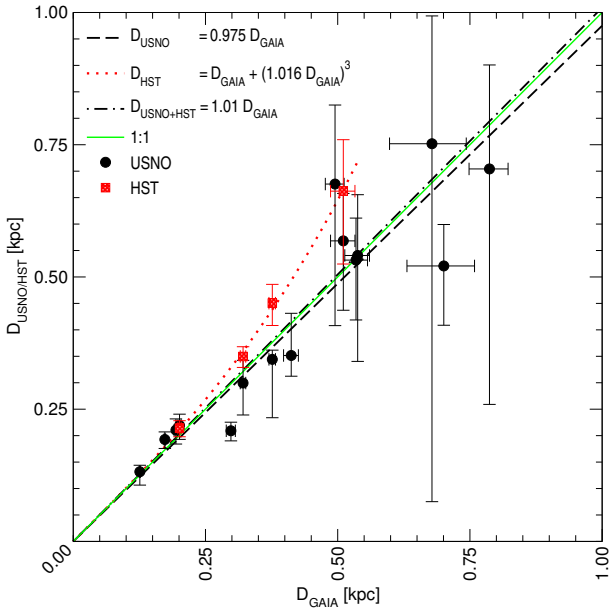

Fig. 1. USNO and HST trigonometric distances vs. GDR2 distances. The linear regressions show the USNO data set alone (dashed line) and the combined data set (dash-dotted line). The HST data set alone is best fit by a relation adding a third-order correction term (dotted curve). The thin green line gives the 1:1 relation.

3.2. Statistical distance scales

As the trigonometric distances are restricted to nearby objects and to targets with large radii, and thus well-isolated central stars, we also compared the data set to the matched sources in the two most frequently used statistical distance scales (SH10 and FPB16). For this purpose, the sources were grouped into two subsamples, one with parallax errors given in *Gaia* as being below 15% (81 sources in SH10) and the other with errors between 15% and 25%[1]. Regressions including weights for published statistical errors on individual sources were applied. Through a filtering process that rejected sources over 2.5σ (for the regression, see Fig. 2), we obtained a distance scale that is shorter by about 7–8% than SH10 ($D_{\rm SH10} = 1.076(\pm0.095)\, D_{\rm Gaia}$; rms = 0.53; $R = 0.80$) and about 13% than FPB16 ($D_{\rm FPB16} = 1.133(\pm0.081)\, D_{\rm Gaia}$; rms = 0.38; $R = 0.79$). While the first result does not show a statistically significant difference, the second result differs by more than 1.6σ (Fig. 2). On the other hand, the red filter of *Gaia* exhibits contamination by the Hα+[N II] emission lines (Evans et al. 2018). Thus we find many objects with colors of (bp − rp) above zero (=red), even if they show blue ($B - V$) colors (as the V band is not effected by the Hα+[N II] and the strong [O III] falls just between B and V in the low-sensitivity region). We expect that the central stars of PNe show $-0.65 \leq$ (bp − rp) ≤ -0.25, therefore we excluded in a further iteration all sources beyond this expected color range to test the quality of the parallaxes versus the photometric extraction of the pure stellar source (although we know that we are biased to larger older nebulae and excluded central stars with high extinction)'. This led to very conservative samples of 47 and 45 targets for SH10 and FPB16, respectively. The resulting comparison removes any scaling factor with respect to the SH10 sample ($D^{\rm blue}_{\rm SH10} = 1.013(\pm0.082)\, D^{\rm blue}_{\rm Gaia}$; rms = 0.47; $R = 0.87$) and has smaller differences with FPB16 ($D^{\rm blue}_{\rm FPB16} = 1.076(\pm0.081)\, D^{\rm blue}_{\rm Gaia}$;

[1] This does not include any of the peculiar objects from Sect. 4.3.4 in FPB16.

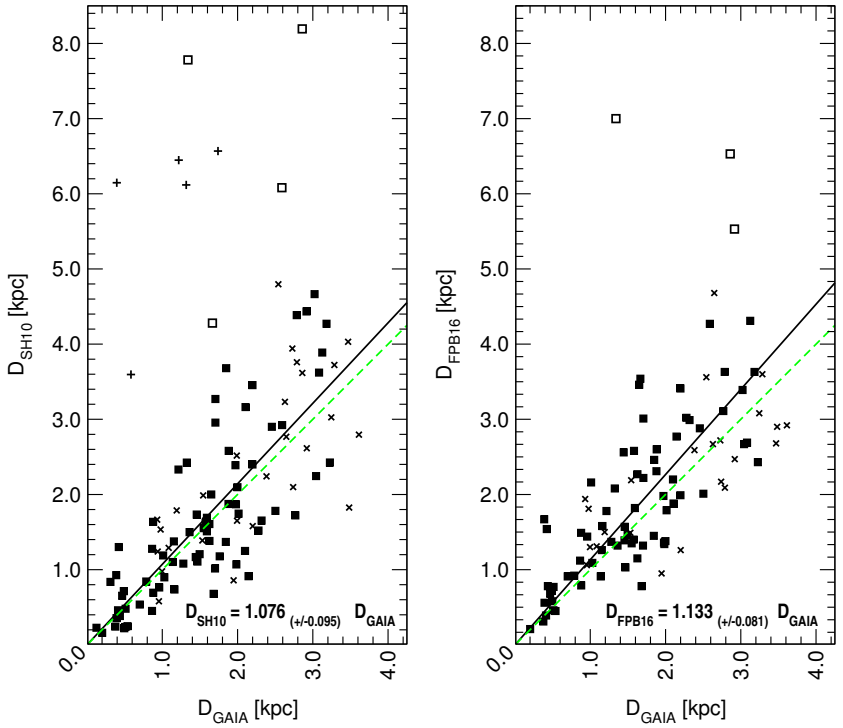

Fig. 2. Comparison with statistical distance scales. We show the catalog of distances by SH10 and FPB16 against GDR2 distances. Filled and empty squares show the data for targets with $\sigma_\pi/\pi < 0.15$ in *Gaia*, where open symbols indicate the sources that we did not use for the regression (2.5σ filtering). The black solid lines show the linear regression of these sources forced through the coordinate origin. Crosses and pluses are used for targets with $0.15 \leq \sigma_\pi/\pi < 0.25$, (the latter were not included in the fitting), where filtered sources are marked with a plus. The fitting including sources with $\sigma_\pi/\pi > 0.15$ marginally changed the result within the line widths and thus is not shown separately for clarity. The green dashed lines show the 1:1 relation.

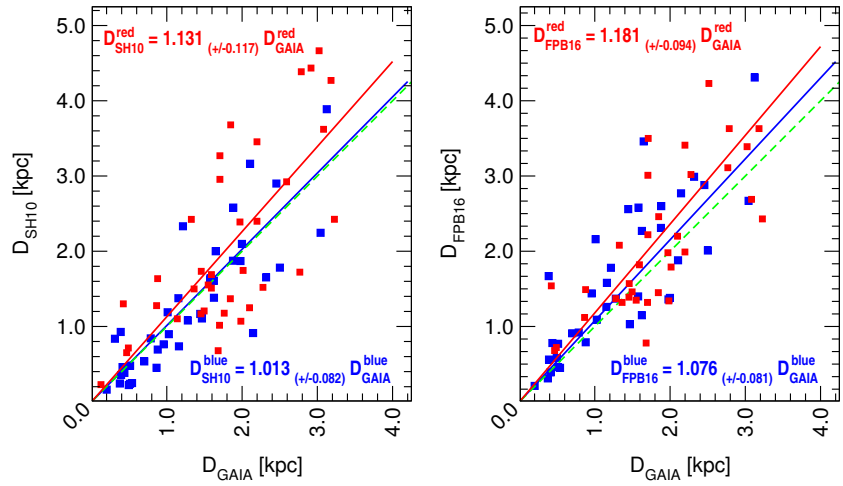

Fig. 3. Comparison with statistical distance scales using only sources with blue colors in *Gaia* (bp − rp) < $-0^{\rm m}.25$ (fit line and symbols in blue) and red objects (fit line and symbols in red). Symbols and lines are the same as in Fig. 2. Sources that we did not use for fitting ($\sigma_\pi/\pi > 0.15$ and the clipped ones) are not shown for clarity.

rms = 0.31; $R = 0.81$), as we show in Fig. 3. For comparison, the fit using only the red sequence targets gives systematically higher inclinations where $D^{\rm red}_{\rm SH10} = 1.131(\pm0.117)\, D^{\rm red}_{\rm Gaia}$; rms = 0.54; $R = 0.72$ and $D^{\rm red}_{\rm FPB16} = 1.181(\pm0.094)\, D^{\rm red}_{\rm Gaia}$; rms = 0.39; $R = 0.75$. More data collected over longer timescales might overcome part of these restrictions. Some targets have still fewer (`visibility_periods_used<10`) than the 15–20 periods available for most sources in the GDR2 catalog and the limit of 8 that is required to be selected for the catalog.

3.3. Radio and optical surface brightness versus radius: *Gaia DR2 versus Gaia DR1/TGAS*

By using the parallaxes from the first *Gaia* Data Release (*Gaia* DR1), Stanghellini et al. (2017) obtained a preliminary recalibration of the statistical distance scales using the surface brightness. They presented a correlation based on a few sources within the TGAS solution, and combined it with the same USNO data set we used here. With these data sets they revisited the calibration schemes of Hβ surface brightness versus radius (derived from parallaxes), and the calibration of radio brightness temperature versus radius. The first method is very similar to the ansatz of FPB16, who used Hα instead. For comparison purposes, we used exactly the same sources to provide a maximum of compatibility from our new data set. We therefore also excluded the halo PN SaSt 2-12 from the fit. The upper panel of Fig. 4 shows that the regression we find with GDR2 has about the same correlation coefficient, but a much lower inclination than they found. For the radio surface temperature method (van de Steene & Zijlstra 1994) we also derived the relation (lower panel of Fig. 4) using all our data from the sample selected from SH10 presented above. We intentionally did not restrict the selection to the blue sample to avoid bias. The results from this full sample are nearly identical to the results found including only the targets used in the previous study. FPB16 was not used, as recalculating from Hα to Hβ, might suffer systematic errors from extinction correction. The differences between our GDR2 calibrations of statistical distance scales and the calibration derived from TGAS are striking. Moreover, as the tests in the previous section have shown, possible caveats for GDR2 parallaxes towards

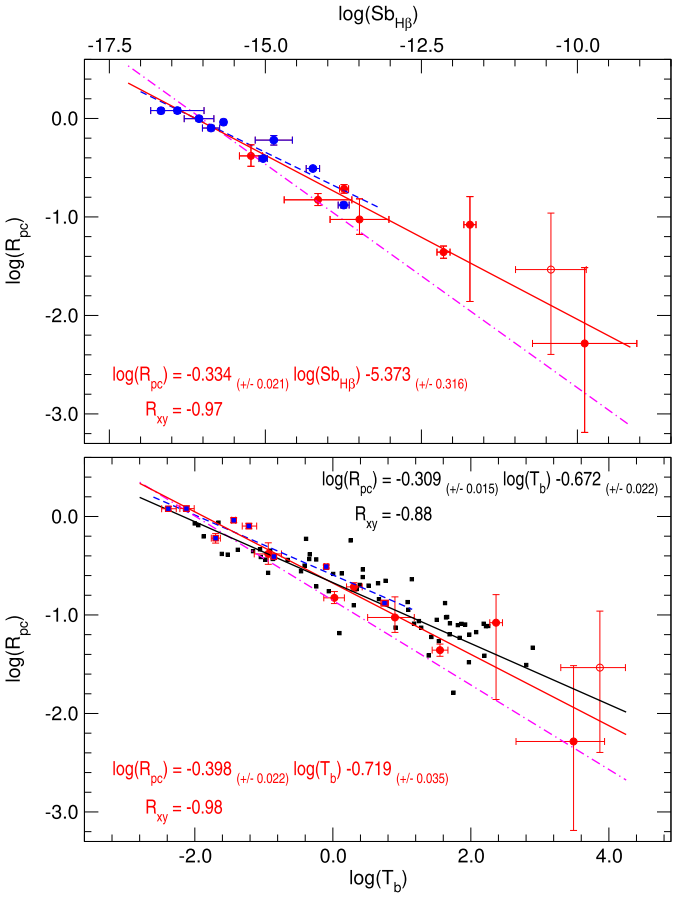

Fig. 4. Comparison with the calibration of Stanghellini et al. (2017). The red symbols show targets with TGAS parallaxes, the blue symbols represent the USNO targets, and black symbols show our larger sample based on SH10. Red fit lines use the same targets as in the previous study, but using GDR2 distances. The black fit line uses the complete sample based on SH10. SaSt 2-12 is marked with an open symbol. The dash-dotted magenta lines show the fits by Stanghellini et al. (2017).

high surface brightness objects with nebular contamination exist.

4. Conclusions

With a cross-identification that was not only coordinate based, we have studied a selected sample of 382 Galactic planetary nebulae from the sample of 728 sources in the distance-scale study of Stanghellini et al. (2008), listed in Stanghellini & Haywood (2010). The selected sample included only targets with a clear identification match to the second *Gaia* release data set. Of these matched sources, 57 have formally negative parallax values and despite good photometric values, 39 have no astrometric solution or parallax at all. Of these 96 sources, 86 have extremely red colors, which is not expected even for the ionizing source of a young planetary nebula.

The remaining sample shows a perfect match of the distance scale to the previous ground-based USNO parallaxes of Harris et al. (2007), with greatly reduced uncertainties. However, the pure HST-based data set by Benedict et al. (2009) clearly shows a systematic high-order error term at distances above 0.35 kpc. All of these targets have blue *Gaia* colors ($0\overset{m}{.}65 < (bp - rp) < 0\overset{m}{.}25$). The comparison with the statistical distance scale from Stanghellini et al. (2008) shows a nearly perfect match, up to the distances of 4 kpc we studied here, when the lists are restricted to the central stars that also reveal blue target colors. Red targets with strong nebular contamination, on the other hand, show some systematic scale factor and much larger scatter than would be assumed given the formal error in the GDR2 data base. For a detailed discussion of the formal error versus real errors, including systematic errors due to a software bug for bright sources ($G < 13$) and the slightly negative zero-point, we refer to Lindegren et al. (2018) and Luri et al. (2018). We thus conclude that the released data systematically underestimate the errors for objects with emitting circumstellar material or high-brightness nebulosity. This will certainly also affect the interpretation of GDR2 data in star-forming regions and OB associations.

As FPB16 have pointed out, parallaxes generally suffer from the L–K bias (Lutz & Kelker 1973). The correction given there assumes a constant error σ_π and thus a steady increase in fractional error $f = \sigma_\pi/\pi$ at larger distances (we used a constant $f < 0.15$) and a constant space density. Neither of these apply here, therefore a detailed study with Monte Carlo simulations similar to those for stars (Luri et al. 2018) has to be done. Nevertheless, this requires a model for the spatial distribution as well as a model of the discovery probability variations in the Galaxy. A comparison with the same sample as was used for a similar study with *Gaia* DR1/TGAS data by Stanghellini et al. (2017) shows strong systematic effects, leading us to conclude that these solutions from TGAS should not be used for stars that are surrounded by strong emission nebulae. However, although it was not restricted to the better parallaxes, our newly derived correlation has to be used with care because of bias effects.

Acknowledgements. This work has made use of data from the European Space Agency (ESA) mission *Gaia* (https://www.cosmos.esa.int/gaia), processed by the *Gaia* Data Processing and Analysis Consortium (DPAC, https://www.cosmos.esa.int/web/gaia/dpac/consortium). This research has made use of the SIMBAD data base and the ALADIN applet, operated at CDS, Strasbourg, France. D.B. was supported by FONDO ALMA-Conicyt Programa de Astronomía/PCI 31150001.

References

Acker, A., Marcout, J., Ochsenbein, F., et al. 1992, The Strasbourg-ESO Catalogue of Galactic Planetary Nebulae. Parts I, II. (Garching, Germany: ESO), 1047
Acker, A., Fresneau, A., Pottasch, S. R., & Jasniewicz, G. 1998, A&A, 337, 253
Benedict, G. F., McArthur, B. E., Napiwotzki, R., et al. 2009, AJ, 138, 1969
Bojičić, I. S., Parker, Q. A., & Frew, D. J. 2017, IAU Symp., 323, 327
Bonnarel, F., Fernique, P., Bienaymé, O., et al. 2000, A&AS, 143, 33
Cahn, J. H., Kaler, J. B., & Stanghellini, L. 1992, A&AS, 94, 399
Daub, C. T. 1982, ApJ, 260, 612
Evans, D. W., Riello, M., De Angeli, F., et al. 2018, A&A, 616, A4
Frew, D. J., Madsen, G. J., O'Toole, S. J., & Parker, Q. A. 2010, PASA, 27, 203
Frew, D. J., Bojičić, I. S., & Parker, Q. A. 2013, MNRAS, 431, 2
Frew, D. J., Parker, Q. A., & Bojičić, I. S. 2016, MNRAS, 455, 1459
Gaia Collaboration (Brown, A. G. A., et al.) 2016, A&A, 595, A2
Gaia Collaboration (Brown, A. G. A., et al.) 2018, A&A, 616, A1
Hambly, N. C., MacGillivray, H. T., Read, M. A., et al. 2001, MNRAS, 326, 1279
Harris, H. C., Dahn, C. C., Canzian, B., et al. 2007, AJ, 133, 631
Kwitter, K. B., Jacoby, G. H., & Lydon, T. J. 1988, AJ, 96, 997
Lindegren, L., Hernandez, J., Bombrun, A., et al. 2018, A&A, 616, A2
Luri, X., Brown, A. G. A., Sarro, L. M., et al. 2018, A&A, 616, A10
Lutz, T. E., & Kelker, D. H. 1973, PASP, 85, 573
Majaess, D. J., Turner, D. G., & Lane, D. J. 2007, PASP, 119, 1349
Majaess, D., Carraro, G., Moni Bidin, C., et al. 2014, A&A, 567, A1
Michalik, D., Lindegren, L., & Hobbs, D. 2015, A&A, 574, A115
Skrutskie, M. F., Cutri, R. M., Stiening, R., et al. 2006, AJ, 131, 1163
Smith, H. 2015, MNRAS, 449, 2980
Stanghellini, L., & Haywood, M. 2010, ApJ, 714, 1096
Stanghellini, L., Shaw, R. A., & Villaver, E. 2008, ApJ, 689, 194
Stanghellini, L., Bucciarelli, B., Lattanzi, M. G., & Morbidelli, R. 2017, New Ast., 57, 6
van de Steene, G. C., & Zijlstra, A. A. 1994, A&AS, 108, 485
Weinberger, R. 1977, A&AS, 30, 343